Tone Production of the Wurlitzer and Rhodes E-Pianos

Florian Pfeifle and Malte Münster

Abstract Two idiomatic examples of electro-acoustical keyboards played since the 60s to the present day are the Wurlitzer E-Piano and the Rhodes E-Piano. They are used in such diverse musical genres as Jazz, Funk, Fusion or Pop as well as in modern Electronic and Dance music. Their unique sound, that is comparable on a generic level, shows distinctive varieties in timbre and decay characteristics. This can be attributed to their specific mechanical-electromagnetic/electrostatic tone production. In this treatise, a description and comparison of the tone production mechanisms are presented based on measurements taken on both instruments, a Rhodes Mark II and a Wurlitzer EP300. The measurements include high-speed camera measurement and tracking of the primary mechanical sound production mechanisms as well as audio recordings of the unamplified instrument signal. It is highlighted that the different timbre can be attributed to different characteristics of the pickup systems of both instruments. In the case of the Rhodes, characteristic sound properties emerge due to the interaction of the mechanical motion of a small tine interacting with the magnetic field (H-field) of the pickup. In the case of the Wurlitzer a vibrating steel reed acts as the zero potential electrode of a capacitor inducing an alternating current due to changes in the electro-static field (E-field). The measurements are compared to a FEM model of the respective geometry showing good accordance with the proposed effects. A simplified physical model is proposed for both instruments along with a more complete physical model taking the geometry of the sound production mechanisms of the instruments into account.

F. Pfeifle (✉) · M. Münster
Institute of Systematic Musicology, University of Hamburg,
Neue Rabenstrasse 13, 20354 Hamburg, Germany
e-mail: florian.pfeifle@uni-hamburg.de

M. Münster
e-mail: m.muenster@arcor.de

A. Schneider (ed.), *Studies in Musical Acoustics and Psychoacoustics*,
Current Research in Systematic Musicology 4,
DOI 10.1007/978-3-319-47292-8_3

1 Introduction

The technological advances in the 19th century that put a mark on many areas of human culture and modern living had, and still have, an formative influence on music production, processing and perception. The utilisation of principles from natural science for sound producing as well as sound modification purposes has a long tradition in different musical styles and genres of the 19th and 20th century. And both areas, music and science, influenced each other in several regards. There are several illustrious examples of electromechanical effects being utilised in the tone production of music instruments, see for instance Hammond organs or early synthesizers.

Today, the majority of keyboard instruments make use, more or less, of digital sound generation, either utilising special sound producing chips or using sampled sound libraries. Nonetheless, and this is somewhat remarkable, many of the digital sounds available in modern keyboards and synthesizers are based on analog instruments either completely acoustic, electro-mechanic or analog-electronic, pointing to a certain preference by musicians as well as music consumers. Thus, a faithful reproduction of those originally analog sounds can help to enhance the musical as well as artistic experience of such sound synthesis methods. The electro-mechanic effects on the other hand can be used to illustrate physical principles of such tone-production, and pickup mechanisms, showing how the characteristic timbre of such instruments is created by utilising fundamental principles of electrodynamics.

In this treatise, two idiomatic examples of electromechanical keyboard instruments are presented. Among two of the most popular “E-Pianos” are the Wurlitzer EP200 and the Rhodes Mark-I/Mark-II pianos, still highly valued among musicians, music producers and evoking specific associations among listeners regarding their specific genre, which primarily is Jazz, Funk and Soul music.

Throughout the following pages, a focus is put on the primary sound production mechanism of both instruments and it is shown that their characteristic timbre is due to the specifics of the respective conversion mechanism of the mechanical motion into an electronic signal, in both cases an alternating current. The influence of the electronic circuit following the basic sound pickup system is left out of the consideration here because the most characteristic part of the instruments sound is produced at the pickup mechanism as will be shown in the following.

The acoustic research history on both instruments is comparably sparse [1,2] and the effects which are published in patent specifications of the respective instrument omit some specific properties of the mechanism and an influence of certain parameters [3]. In this treatise we want to elucidate the mechanisms to aid the development of a physical model for sound synthesis and auralisation of both instruments.

After a short historic overview, the physical effects of both tone production mechanisms are described and a series of measurements are presented along with a consideration of the influences of the investigated effects. These are combined to a simplified model of the instrument, implemented using finite difference schemes

and a more elaborate model of both instruments taking the specific geometry of the instruments pickup mechanism into account.

2 History

In this section a short overview on the history and the evolution of both instruments is given, a focus is put on the inventions surrounding the primary sound production of the instruments.

2.1 History of the Rhodes

An early electromechanical instrument was constructed by Thaddeus Cahill (1867–1934) in 1906. The *Dynamophone* or *Telharmonium*, a vastly huge organ instrument with motor driven wheels having different profiles. The rotating, later called tonewheels induce a change in voltage in a magnetic field of a wire coil around a permanent magnet, following to their profiles. This idea delivered the conception for Laurens Hammond's successful organs. It is directly referable to the principle of the AC-generator from 1832 by Antoine-Hippolyte Pixii (1808–1835).

The first commercially successful application was an electrical phonograph pick up, introduced in the 1920s. The first obtainable musical instrument with such a pick up were Rickenbacker's Hawaiian lap guitars A22/A25 (known as Frying Pan), developed by George D. Beauchamp 1932 [4, 5]. The earliest known piano like instrument using an electromagnetic pick up was the Neo-Bechstein piano, a modified acoustic grand piano using pickups to capture string motion and subject it to electronic modification and amplification. It was conceived by Walther Nernst in 1930, together with the companies Bechstein and Siemens. In 1940 Earl Hines started touring with a RCA Storytone Electric Piano, a comparable construction being sold in the U.S. [6].

The Rhodes electric piano was invented by Harold Burroughs Rhodes (1910–2000). As a piano teacher he developed his own teaching method. During World War II he invented the Army Air Corps Piano to enable recovering soldiers to play piano. It was a miniaturised acoustic piano using aluminium tubing instead of strings to produce a xylophone-like sound much like a toy piano. After the war, H. Rhodes founded the Rhodes Piano Corporation to built and sell a more advanced instrument, the Pre-Piano with a new electromagnetic tone production [7, 8]. Leo Fender, already a big name in making and marketing electric guitars and amplifiers, acquired the Rhodes Piano Corporation in 1959. The first model was the Rhodes Piano Bass. The generator part now included a so called Rhodes Tuning Fork [9]. The assembly was refined to produce an intense fundamental tone, lacking higher harmonics. Under the leadership of CBS who bought out Leo Fender 1965, sales were enforced. Gaining popularity in several genres of popular music originating from jazz music,

the Rhodes piano became the largest-selling electronic piano until the end of production 1983 due to upcoming, affordable polyphonic synthesizers and samplers. Since the 1990s, the instrument enjoyed a resurgence in popularity. From 2007 on it has been reissued by the Rhodes Music Corporation as Rhodes Mark 7.

The standard models Mark-I and Mark-II did not came with pre-amplifiers, their electronics are passive, comparable to most electric guitars. Among a few works' own solutions like the Rhodes Janus I -P.A.-system, the suitcase models with built-in amplifiers and the Fender Twin Reverb, the Roland Jazz Chorus-Line of guitar amplifiers are common amplifier choices for stage and studio.

2.2 *History of the Wurlitzer*

In contrast to the history of the Rhodes Piano the conditions and circumstances were different in the case of the Wurlitzer E-piano. While the first Rhodes Pianos were produced under the leadership of a young, small but famous Californian guitar manufacturer, which had no experience in making keyboard instruments at all, the Rudolph Wurlitzer Company Ltd. (1853–1985) started as a retailer of stringed, woodwind and brass instruments from Germany and supplied U.S. Military bands. In 1880 the company began manufacturing acoustic pianos. Later, they were very successful in making band organs, *orchestrions*, *nickelodeons*, jukeboxes as well as theatre organs.

Most tone production mechanism of the aforementioned instruments are based on mechanical principles, whereas the Wurlitzer E-piano series makes use of an electrostatic pickup system. The company had some preliminary experience in the use of this technique. After world War II, Wurlitzer acquired the Everett Piano Company who manufactured the *Orgatron* which was an electrostatic reed organ developed by organist and conductor Frederick Albert Hoschke in 1934. Wurlitzer kept the Orgatron in production until the mid-1960s. The pickup mechanism of Wurlitzers electrostatic organs and pianos lie in the same plane as the vibrating reed, opposed to the U.S. patent which includes a description of such a construction with extended "ear like" metal plates [10], whereas later models omit these "ears". The principles of electrostatic pickups were patented by Benjamin F. Miessner in the U.S. [11] and at about the same time by Oskar Vierling in Austria and Germany 1932 [12, 13]. Their supposedly common research led to the *Elektrochord*, a string based piano with electrostatic pickups [6].[1]

[1]There are speculations about earlier electrostatic pickup system supposedly developed by sound engineer and luthier Lloyd Loar while he worked for the Gibson Guitar Company from 1919–1924. There are no designs preserved from this time nor are there schematic drawings which would substantiate this assumption [14] but at least one of the original Loar-designed L5s from 1929 was factory fitted with an electrostatic pickup [15] which was incorporated into the resonance body of the guitar thus picking-up only body vibrations and not the vibrations of the strings as electromagnetic pickups do.

The first electronic piano consisting of a comparable pickup system as modern Wurlitzer E-pianos was the Model 100 marketed in 1954 [16]. This early instrument was followed by a series of similar models, the EP110, EP111, EP112 which had several small differences and enhancements compared to the earliest model but had a similar tone production mechanism. All Instruments had pre-amplifiers and small power amplifiers to drive built-in speakers. The pre-amplifier includes patented high- and low-pass filtering; later transistorised models had local negative feedback within the circuitry to suppress system immanent noise produced by the sensitive tone generator. Including all variations and different sub-models there supposedly exist between 40 and 50 models differing in shape, size and/or amplification circuitry [17]. Among these, the most popular Wurlitzer model, manufactured until 1981, is the Wurlitzer EP-200A. This model, which typically consists of a black plastic body, incorporates an amplifier and two small speakers built into the casing and facing the player. Similar to earlier models it consists of a tremolo sound effect which can be gradually added to the amplified sound of the instrument.

3 Physical Properties

In this section an overview of the physical properties of the instruments measured in this work is given. A focus is put on primary sound production mechanisms of the Rhodes and Wurlitzer electronic pianos and their respective tone production geometries.

3.1 Sound Production of the Fender Rhodes Electric Piano

The sound production of the Fender Rhodes piano can be divided into two parts, a mechanical part and an electromagnetic part.

The mechanical part consists of a rod made of spring steel shrunk into an aluminium block on one side, making the resulting system comparable to a cantilever beam. The length and circumference of the rod as well as the position of a small tuning spring, adding mass, determines its fundamental frequency. The rod, which in the case of the Rhodes piano is called a tine, is excited by hammer that has a neoprene tip. The key action mechanism is a simplified single action as described in [18], it can be compared to a *Viennese* or *German* piano action because the hammer is in direct contact with the key. Depending on the year of construction the key and hammer mechanisms are crafted from wood or, as generally used in newer models, of synthetic materials. Every tine is damped by an individual felt damper that is in contact with the tines from below. The fixation of the tine, the aluminium block, is tightly connected to a, sometimes $\frac{pi}{2}$ twisted, brass bar which acts as the second prong of the patented Rhodes' "tuning fork" system.

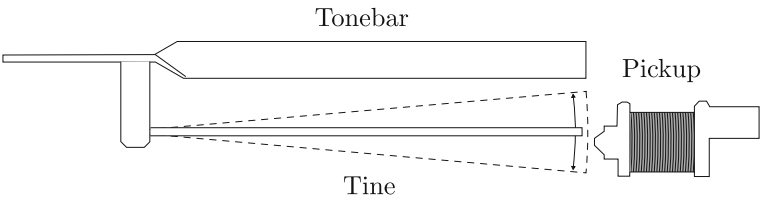

Fig. 1 The Rhodes tuning fork assembly with electromagnetic pickup

When played softly, the sound of a Rhodes piano can be described as *glockenspiel*-like, consisting of an extremely short transient showing higher, non-harmonic partials quickly leading to a quasi stationary waveform after 10–30 ms. As shown in (isma/jasa), the higher non-harmonic partials are created by the brass bar and are more prominent in the upper register of the instrument.

Depending on the velocity of the attack, lower notes tend to have a rich harmonic sound characteristic, often described as a "growling" sound. By playing more softly, the fundamental frequency of the tine vibration is more present, by gradually increasing the playing force the sound becomes successively more "growly". This playing characteristics adds to the Rhodes piano's expressivity as a music instrument.

The harmonic oscillations of the mechanic part of the Rhodes' tone production is converted to an alternating voltage by an electromagnetic pickup, that consists of a wound permanent magnet comparable to a pickup of a guitar in its overall structure but differing in terms of the magnets geometry as is depicted in Fig. 1. It consists of a round ferrite permanent magnet attached to a frustum made of iron. The magnet is wound by a coil consisting of ≈2500–3000 turns of 37 AWG[2] enamelled wire running on a synthetic bobbin.

The geometry of the pickup's iron tip shapes the specific distribution of the magnetic field in which the tine vibrates. The motion of the ferromagnetic tine changes the flux of the magnetic field which in turn produces a change in the electromotive force of the pickup resulting in an alternating voltage which then can be amplified by an external amplifier. The copper wire winding of each pick up is divided into two sections, connected in opposite phase for hum cancelling. The sound of a tone can be altered by changing the position of the tine in respect to the magnet. The more a tine is aligned towards the center of the wedge shaped magnet the more symmetrical the resulting waveform is. When aligned perfectly centered, the produced sound behind the pickup is twice the fundamental of the tine as schematically depicted in Fig. 17a. The more the tine is shifted towards the edge the more asymmetric the resulting sound is, leading to a higher amount of harmonic partials which is classified as "growl" by most musicians. The influence of this effect is represented in Fig. 17b. In higher registers, the Rhodes' tine is smaller thus having a smaller deflection which results in a smaller change of the magnetic flux

[2]American Wound Gauge.

and the resulting sound has a stronger fundamental without a comparable amount of higher partial as lower notes tend to have.

3.1.1 Measured Instrument

The instrument measured for this treatise is a Rhodes Mark-II stage piano consisting of 73 keys. It is equipped with synthetic hammers with a neoprene tip which is the typical material choice for Rhodes E-piano hammers since the mid-70s. The keys themselves are made of wood.

3.2 Sound Production of the Wurlitzer EP300

In contrast to the Rhodes' electromagnetic pickup system, the Wurlitzer piano sound production utilises electrostatic effects. A steel plate that is impacted by a hammer vibrates as an electrode of a capacitor resulting in a time varying capacitance. The plate, called reed in the user manual of Wurlitzer pianos [19], is made of hardened light spring steel, fixed at one end and free at the other. There are two factors determining the fundamental frequency f_0 of every reed, the physical dimensions of the reed itself and the amount of solder on the tip of the reed. By removing or adding lead to the tip of the reed its f_0 is increased or lowered respectively. As shown in Fig. 2, a voltage of 170 V is applied to a stationary plate and the reed acts as the low potential electrode of the resulting capacitor. The charged plate has cutouts at the position of the reed for each note of the instrument. The reeds are able to vibrate freely between the symmetric cutouts, providing a surface area large enough to produce a measurable change in capacity. The air gaps between plate and reed act as dielectric material. Analogous to the case of a plate capacitor or the diaphragm of a condenser microphone, the capacity varies inversely proportional to the distance between the two electrodes, here, reed and fixed plate.[3]

The key action mechanism of the Wurlitzer piano consists of a miniaturized London style piano action that can be regulated like a grand piano action. Every reed of the Wurlitzer piano is excited by an individual ply maple hammer that has a felt tip [19]. Comparable to the playing dynamics of the Rhodes E-piano, depressing the keys with higher velocity results in a richer harmonic sound of the Wurlitzer than playing softly.

[3]As side note it should be mentioned that Miessner proposed an electrostatic pickup using high-frequency AC to pre-load the capacitor system to avoid non-linear distortion of large displacements of lower sounding, larger reeds, Wurlitzer instead choose to set the DC pre-load high enough to keep the E-field large to prevent effects of distortion.

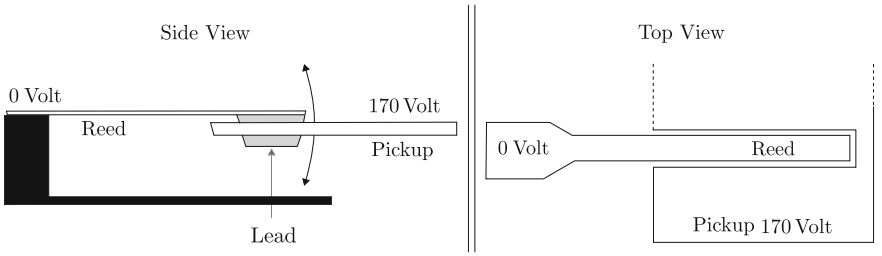

Fig. 2 Structural depiction of the Wurlitzers pickup system. A side view on the *left*, top view on the *right*. Both showing the high potential plate and the low potential reed

3.2.1 Measured Instrument

The Wurlitzer piano model measured in this treatise is a Wurlitzer EP300 which has an amplification circuitry which is a mixture of the popular EP200A and the EP140 and is a model which was only marketed in Germany. The tone production is similar to the EP200 series, but, in comparison to the synthetic case of the EP200A it consists of a ply wooden case containing three integrated speakers as well as individual inputs and outputs for head-phones, external speakers or microphones. Comparable to most Wurlitzer piano models it consists of 64 keys ranging from A1 with a fundamental frequency of 55 Hz to C7 with a fundamental frequency of 2093 Hz.

Contrary to the values given in Wurlitzer's service manual schematics, a measurement of the high potential plate of this instrument shows ≈147 V and not 170 V, as indicated in the manual. Shown in Fig. 3 is the resistor where the direct-out voltage is measured. The physical properties of the reeds of this instrument are given in Fig. 4 and Table 1.

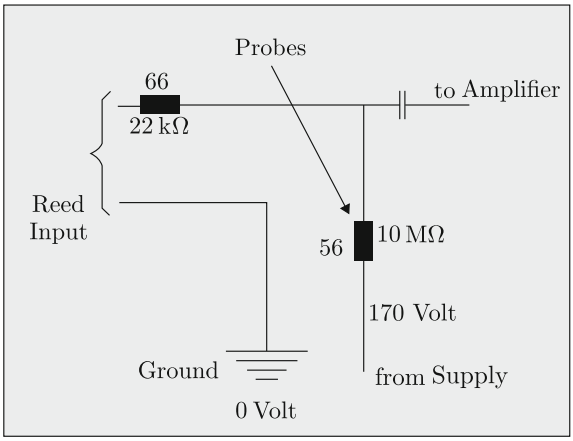

Fig. 3 Section from the Wurlitzer EP300 schematic. Indicated by the *arrow* the resistor where the electric probe measurements are performed

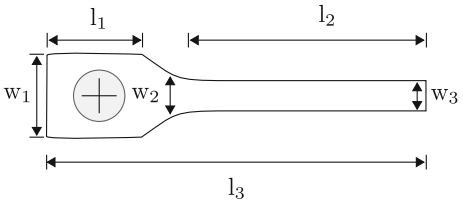

Fig. 4 Length indexes for the values given in Table 1. The speaking length l_2 is the portion of the reed not in contact with its mounting

Table 1 Physical sizes of Wurlitzer reeds

	Base length (l_1)[a]	Speaking length (l_2)	Total length (l_3)	Total width (w_1)	Base width (w_2)	Tip width (w_3)
Lowest reed	13	61	74	10	6.7	4
Highest reed	13	13	27	10	2.8	2.5
measured reed	13	47	62	10	6.5	3.8

[a]All values in [mm]

The tines are fixed by screws at their base shown in Fig. 4. The contact point between hammer and the Wurlitzer's reeds is approximately at half the reed's speaking length. The impact point between hammer and the measured reed is at 22.27 [mm] from the tip which is approximately half its speaking length.

4 Methods

To characterise the exact influences of different parts belonging to the tone production, a set of measurements are performed using different methods. All measurements presented here are carried out at the Institute of Systematic Musicology at the University of Hamburg.

4.1 Camera Tracking

A high-speed camera is used to qualitatively record visibly moving parts of the instrument, and to track specific motions of the respective parts. In the case of the Rhodes E-piano, the motion of a freely vibrating tine as well as a hammer impacted tine vibration. In the case of the Wurlitzer EP200, the motion of a hammer impacted reed vibration is recorded and tracked. For all measurements, a *Vision Research Phantom V711* high-speed camera is applied. For recording and qualitative evaluation of the high-speed recordings, the Vision Research *Phantom Camera Control*

Fig. 5 A typical section of a high speed camera recording setup showing part of the Rhodes' tine including the tuning spring and the electromagnetic pickup. The tip of the tine is marked with *black ink* to facilitate motion tracking. In a realistic scenario, gain, luminosity and contrast of the camera recording are changed to emphasize tracked points

software version 1.6 and 2.7 is used. For evaluating the recording quantitatively, the *Innovision Systems* motion tracking software *MaxTraq2D* is applied. The traced trajectories are exported to an ASCII-format file, and analysed with scripts coded in *julia* language, using wavelet methods as well as Fourier transform analysis.

The measurement setup consists of the high-speed camera, a set of LED lamps and the device under test which is marked with white or black ink at several points on the geometry to facilitate automatic motion tracking.

A typical image section from a measurement is depicted in Fig. 5.

4.2 Audio Measurements

Audio signals are measured directly after the primary tone production mechanism. The Rhodes piano is equipped with a direct out jack behind the magnetic pick ups. This jack is connected to an audio recording system on a personal computer, recording the alternating voltage with a sampling rate of 44,100 Hz and 24 bit resolution.

The Wurlitzer EP200 does not consist of an output in front of the amplifying circuit, thus, the voltage is measured over a resistor using an electric probe which is connected to a high-precision measuring amplifier and converter sampling at a frequency of 50.0 kHz with a bit depth of 24 bits. The specific resistor is indicated in Fig. 3.

5 Measurements

The measurements are performed on a Fender Rhodes Mark-II and a Wurlitzer EP300. The vibrational behaviour of the sound production assemblies are investigated using high speed camera techniques and audio recordings of the instrument sound immediately following the electromechanical pickup system.

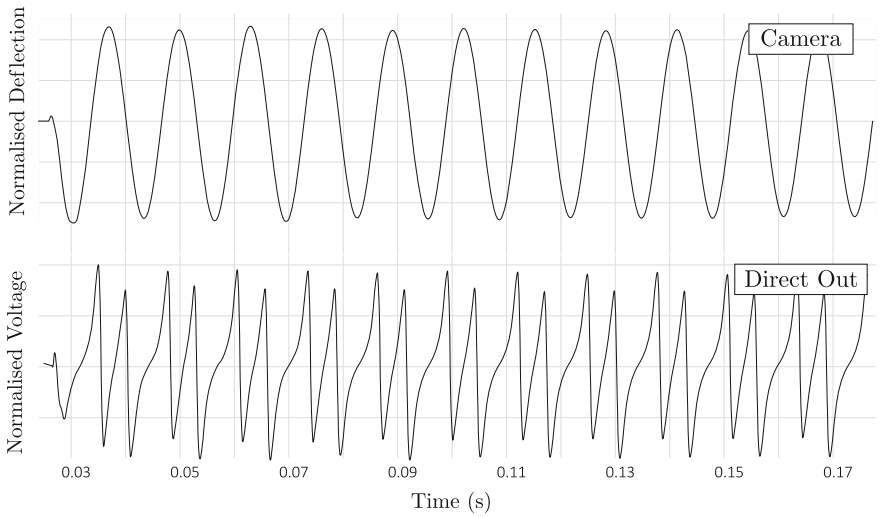

Fig. 6 The *upper graph* shows the tracked signal from a high-speed camera recording of the tine's tip, exhibiting approximately sinusoidal motion. The *lower graph* shows the voltage measured behind the pickup at the direct-out jack of the Rhodes Stages piano

5.1 Rhodes

To characterise the influence of the Rhodes' tine on the resulting sound, several tines are measured using high-speed camera recordings. Figure 6 shows the tracked motion of a Rhodes tine tip with the fundamental frequency of ≈78 Hz and the resulting direct-out sound recorded behind the pickup of the same tone. The note is played *forte*.

The measured signals show that the primary vibrating part of the Rhodes' tone production, the tine, is vibrating in almost perfect sinusoidal motion. The direct-out measurement shows a considerably more complex behaviour pointing to the fact that the magnetic pick up is the main contributory factor of the specific instrument sound. As depicted in Fig. 7 the spectrum of the measured audio signal shows rich harmonic content with a smooth decay of the higher partials and a long-lasting fundamental. A small amount of beating is visible in the first harmonic around the 3 s mark and also in the 4th and 6th harmonic.

To classify the influence of the hammer impact four points in the vicinity of the contact area between hammer tip and tine are recorded and tracked. Figure 8 shows that the hammer impact lasts approximately 4.7 ms and is divided into one longer period and a short reflection, this behaviour is comparable to the occurrence of multiple contacts in low register piano string/hammer excitation []. Comparable to the vibration characteristics of the tine tip, a measurement near the impact point shows sinusoidal motion after approximately one cycle.

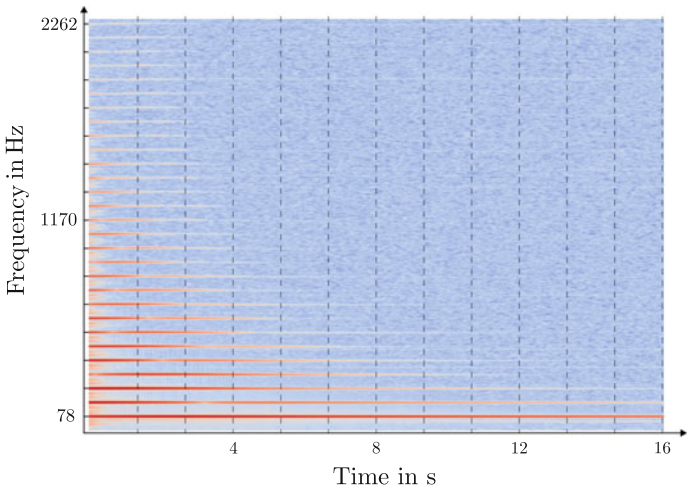

Fig. 7 A spectrogram of the measured audio signal of the Rhodes

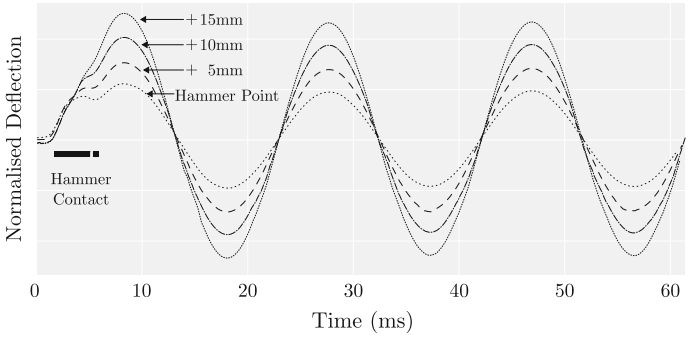

Fig. 8 Four tracked points near the impact zone of the hammer. The *black bar* indicates the contact time between hammer and tine

5.2 Wurlitzer

In this measurement setup, the tip of a Wurlitzer reed excited by a forte stroke is recorded and tracked. Figure 9 shows the tracked motion of a Wurlitzer reed tip with a fundamental frequency of ≈98 Hz under normal playing conditions and the resulting direct-out sound of the same measurement. Corresponding to the measurements of the Rhodes piano, the tip of the Wurlitzer's reed shows an approximate sinusoidal motion whereas the sound recorded behind the pickup exhibits a considerably complex wave form. Again pointing to the fact that the electrostatic pickup is essential for the formation of the specific Wurlitzer sound. As shown in Fig. 10 the recorded audio signal shows a highly complex spectrum with up to 40

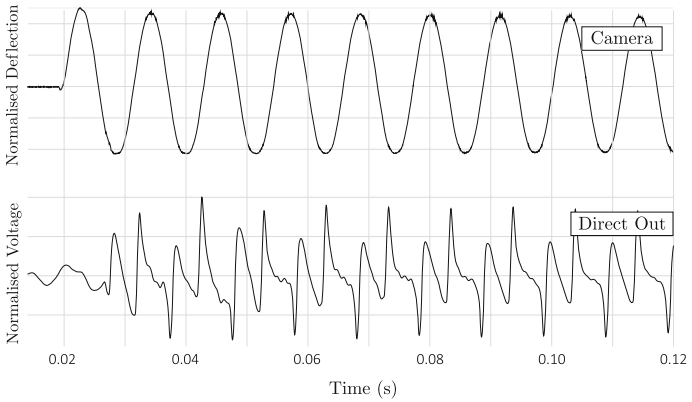

Fig. 9 The *upper graph* shows the tracked signal from the high-speed camera recording again exhibiting approximately sinusoidal motion. The *lower graph* shows the voltage measured behind the pickup over a resistor ahead of the pre-amplification circuitry

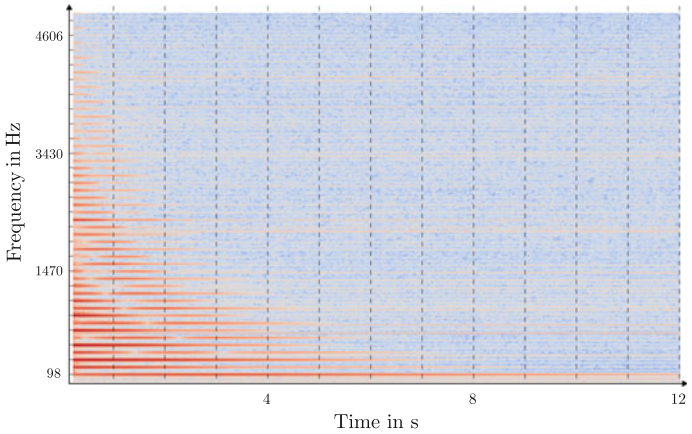

Fig. 10 A spectrogram of the measured audio signal of the Wurlitzer

partials present in the first second of the sound. In addition to the rich harmonic content, the decay characteristics of higher partial show a complex non-exponential decay behaviour with several partials showing a strong beating, e.g. the 3rd and the 5th.

The influence of the hammer is tracked at several points around the impact position. Figure 11 shows that the hammer has a small but noticeable influence on the measured vibration. And the motion is not immediately sinusoidal like the Rhodes tine. The hammer impact lasts around 1.25 ms.

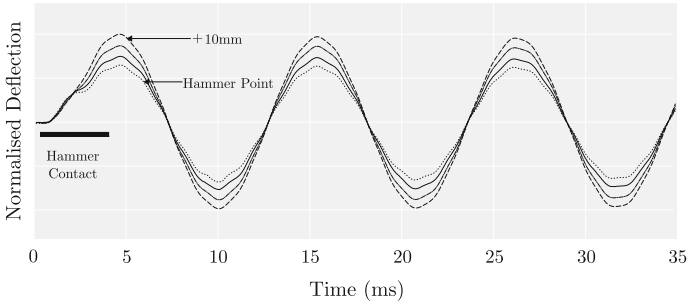

Fig. 11 Four points near the impact zone of the hammer. The *black bar* indicates the contact time between hammer and tine

6 Intermediate Results

The presented measurements of the mechanic part as well as the electronic part of the tone production of both instruments leads us to the intermediate conclusion that the primary mechanical exciters play only a secondary role in the sound production of both instrument and the specific timbre is influenced more by the specific pickup system. In particular the electromagnetic pickup of the Rhodes and the electrostatic pickup of the Wurlitzer. A crucial part of the instruments sound characteristic and timbre must thus be attributed to the coupled electro/mechanical systems at hand. The measurements of both instruments show that the main vibrating parts are vibrating approximately in sinusoidal motion. The resulting sounds measured directly behind the electrostatic or electromagnetic pickup show a more complex behaviour. In the case of the Wurlitzer, the specific pickup geometry leads to a highly complex decay characteristic showing interesting effects like non-exponential decay characteristics and beating of higher partials.

7 Finite Element Models of Sound Production Assemblies

To assess the influence and the specific distribution of the magnetic and electrostatic fields in the vicinity of the pickups [20–22], finite element method (FEM) [23] models of the sound production units of both electric pianos are developed and simulated using the FEM tool and solver *Comsol Multiphysics*.

7.1 Magnetic Field of the Rhodes Pickup

The FEM-model of the Rhodes' pickup system includes the magnetic field surrounding the iron conic section as well as the attached magnet. It is simplified by

omitting the copper coil windings and thus leaving electrodynamic effects out of the consideration. The static magnetic field distribution is computed using a scalar magnetic potential. Assuming a current free region, the relation

$$\nabla H = 0 \tag{1}$$

holds, with H being the magnetic field. Comparable to the definition of the electric potential for static E-fields, the magnetic scalar potential V_m is given by

$$H = -\nabla V_m \tag{2}$$

Using the equivalence $B = \mu 0(H + M)$, and $\nabla B = 0$, where B is the magnetic flux density we can rewrite Eq. 2 to

$$-\nabla(\mu_o \nabla V_m - \mu_o M) = 0\ , \tag{3}$$

with M the magnetization vector describing the magnetization of a material influenced by magnetic field H. Generally M can be seen as function of H [24, pp. 195 ff].

The tine of the Rhodes is positioned in close proximity to the steel tip of the pickup. The flattened sides of the frustum focuses the magnet field in the center showing an approximate bell curve characteristic. The sound is shaped by the distance between the tine and the magnet, caused by the strength of magnetic flux at the respective position. The model shows the disturbance of the magnet field [25]. As the deflection of the tine gets larger, it leaves the magnet field resulting in a more asymmetrical change magnetic of magnetic flux. An idealised model of the pickup system is depicted in Fig. 12 showing a distribution of the static H-field forces surrounding the tip of the magnet.

Geometry of the Pickup Tip

To classify the influence of the pickup shape three models with different tip geometries are created. The resulting H-field in the normal direction of the pickup on a curved line approximately 8 mm above the tip are depicted in Figs. 13 a–c.

As is depicted in Fig. 13a–c, the specific form of the Rhodes' pickup shapes the magnetic field in front of the pickup resulting in a bell shaped curve with different Q-factors.[4]

7.2 *Electrodynamic Interaction of the Wurlitzer Piano*

The FEM model of the Wurlitzer pickup system is developed to solve the dynamic influence of the vibrating reed on the capacitance of the quasi-condenser system. This is achieved by solving Poisson's equation for several static positions on the

[4]The Q-factor is defined as the ratio of the center frequency and the bandwidth. In our case, the center frequency is the position above the symmetry axis of the magnet's tip.

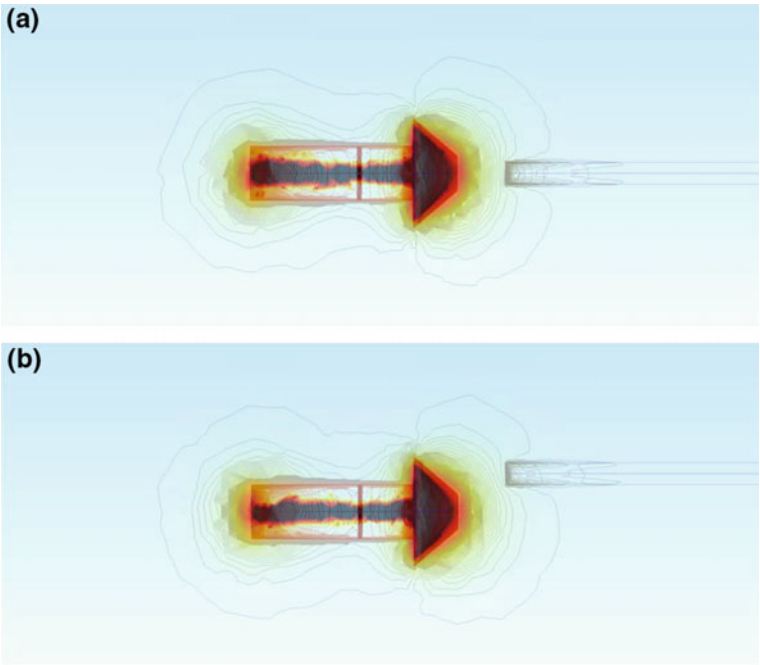

Fig. 12 A FEM simulation of the Rhodes' tine and pickup system showing the resulting force lines due to the magnetic field. The tip of the tine is magnetised as well which is indicated by the force lines on the tine. **a** Symmetric positioning in front of the magnet. **b** Asymmetric positioning of the tine in front of the pickup

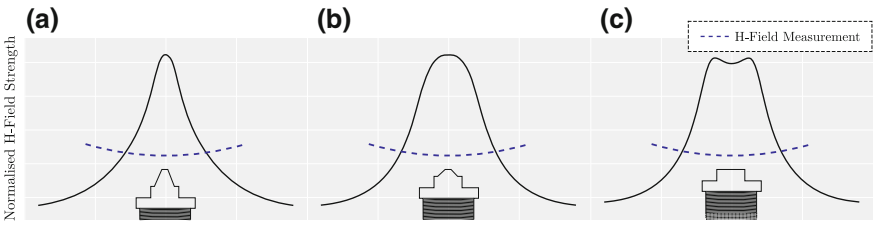

Fig. 13 A FEM simulation of the Rhodes' pickup tip and the resulting H-field strength on a *curve* above the tip. **a** A narrow and high pickup tip and the resulting H-field. **b** A medium high pickup tip and it's resulting H-field. **c** A planar pickup tip comparable to the top of a guitar pickup and the resulting H-field

trajectory of the reed's motion. The stationary electrode of the modeled pickup is charged with a voltage of 147 V whereas the reed is kept at zero potential. The pickup behaves similar to a plate capacitor, where changing distances over time between the reed and the plate results in a changing capacity. A post-processing

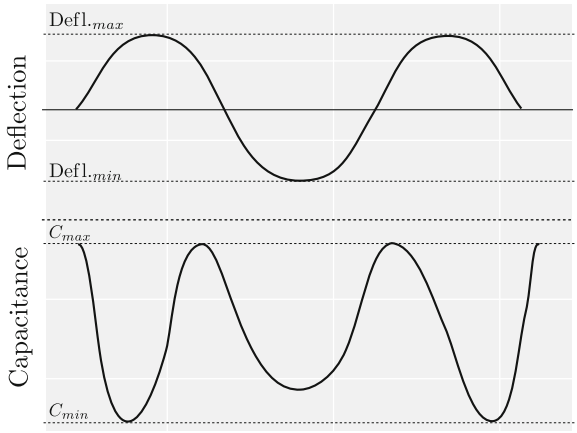

Fig. 14 The changing capacitance due to changing deflection of the Wurlitzer reed

step then computes the change in capacitance. The models work under the following assumptions:

The electric scalar potential, V, satisfies Poissons equation:

$$-\nabla(\varepsilon_0 \varepsilon_r \nabla V) = \rho \tag{4}$$

ε_0 is the permittivity of free space, ε_r is the relative permittivity, and ρ is the space charge density. The gradient of V gives electric field and the displacement:

$$E = -\nabla V D = \varepsilon_0 \varepsilon_r E \tag{5}$$

Boundary conditions of the electric potential are applied to the reed and plates. A potential of 147 V is applied to the plate, whereas the reed maintains grounded. For the surrounding air of, conditions corresponding to zero charge are applied:

$$n \times D = 0 \tag{6}$$

The capacitance of the pickup is changed by the motion of the moving reed. A varying current flows into the plate as needed to maintain the proper charge for a new amount of capacitance. This current produces a varying voltage across an external resistor which is decoupled and amplified to produce a usable output signal as shown in Fig. 3.

The changing capacitance is depicted in Fig. 14. At the capacitance minima of the curve, the excitation of the reed is maximum and at the peaks where capacitance is maximum the reed is near its rest position. Because of the non-symmetric design of the Wurlitzer's reed, the capacity change differs at each excursion depending on moving direction as already measured in 1965 by Ippolito at Wurlitzer Co. [26].

8 Finite Difference Models

The numerical models presented in this section are based on the measured properties presented in Sect. 5, qualitative observations of the FEM models presented before and some conjectures regarding material properties of the Wurltizer's reed and the hammer tip of both instruments. Taking the measurement results as a basis for the models results in several assumptions that simplify the model description of the physical system considerably. Regardless of the introduced simplifications both models are able to capture the vibratory motion and the acoustic properties of both instruments to a high degree while minimizing computational as well as modeling complexity.

A model of both pickup systems including all physical parameters would have to take time-varying electromagnetic effects into account using Maxwell's equations for electromagnetism to describe the respective pickup mechanism in complete form. But, due to the small changes in the magnetic as well as electric fields the proposed simplifications lead to models that are able to approximate the vibratory as well as the sonic characteristics of the instruments very accurately.

The Rhodes models presented here is an extension of the model published in (ISMA 2014) and corrects several shortcomings and imprecise assumptions of this earlier work. The model of the Wurlitzer EP200 shares conceptual similarities with the Rhodes model but is adapted to the different geometry of the sound production. Both models consist of a hammer-impacted resonator exiting a spatial transfer function modeled after the characteristic pickup system of the respective instrument.

8.1 Rhodes Exciter Model

As shown in Fig. 1 the tip of the tine vibrates in close proximity to the electromagnetic pickup and the FEM simulations given in Fig. 12 show that only a small part of the tip is influenced by the magnetic field. Therefore, the exciter of the Rhodes is modeled as a hammer impacted simple harmonic oscillator (SHO) representing the quasi-sinusoidal motion of the tip.

Using Newton's second law, the temporal evolution of a SHO can be written as a second order ordinary differential equation

$$x_{tt} = -\kappa \cdot x \tag{7}$$

with $\kappa = \frac{k}{m}$ the stiffness/springiness of the system, m the mass of the harmonic oscillator, x the deflection and the subscript by t on the left hand side indicating a second derivative in respect to time.

A hammer impact with elastic material properties of the hammer tip can be simulated by using a hysteretic hammer model as presented in [27, 28]. This impact

model is able to simulate hammer impacts of different materials showing viscoelastic behaviour.

Thus, the impacted SHO is extended to

$$x_{tt} = -\kappa \cdot x - F_{\text{int}} \tag{8}$$

with F_{int} the resulting contact force between hammer and SHO, following [27], this force follows the relationship

$$F_{\text{int}}[x(t)] = \begin{cases} k \cdot x(t)^{\alpha} + \lambda \cdot x(t)^{\alpha} \cdot x_t(t) & \text{if} \quad x > 0 \\ 0 & \text{for} \quad x \leq 0 \end{cases} \tag{9}$$

which originally is a model for hammer impacts developed by Hunt and Crossly [29], that has shown to yield good results for models of hammer impacts with moderate impact velocities and plain geometries [27, 30]. Here, α is the nonlinearity exponent depending on the geometry of the contact area and λ is a material dependent damping term that dissipates energy in dependence to the velocity of the changing hammer-tip compression written as x_t.

A typical hammer force over hammer-tip compression curve is plotted in Fig. 15.

The differential equation for both systems can be separated by defining $v = u_t$, the velocity and thus rewritten as

$$\begin{aligned} v_t &= -\kappa \cdot x \pm F_{\text{int}} \\ x_t &= v \end{aligned} \tag{10}$$

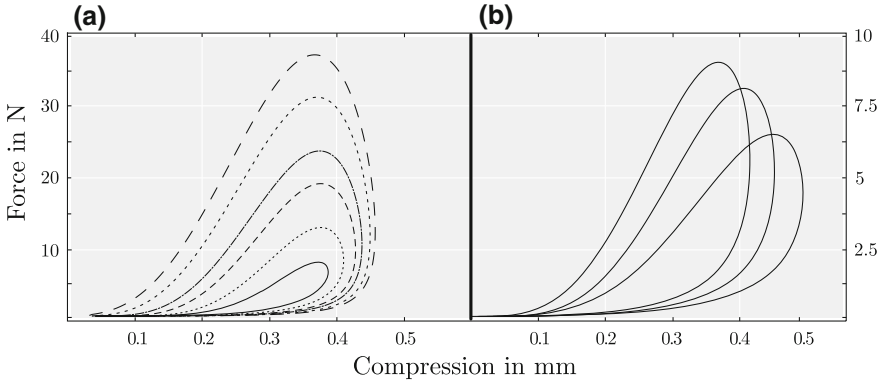

Fig. 15 Force over compression profiles for different hammer parameters. **a** Different values for damping constant λ. **b** Different values for for non-linearity exponent α

8.1.1 Finite Difference Approximation

The exciter models of the Rhodes and the Wurlitzer pianos are discretised applying standard finite difference approximations using a symplectic Euler scheme for iteration in time. The discretisation method and the scheme are published in more detail in [31, 32]. Applying standard FD approximations for the given problem using the operator notation given in Appendix II and iterating the scheme in time by using mentioned method leads to two coupled equations

$$\begin{aligned} \delta_t v_{sho} &= -\kappa_{sho} \cdot x_{sho} - \gamma \delta_t x_{sho} - F_{int} \\ \delta_t x_{sho} &= v_{sho} \end{aligned} \tag{11}$$

for the impacted SHO and

$$\begin{aligned} \delta_t v_{ham} &= -\kappa_{ham} \cdot x + F_{int} \\ \delta_t x_{ham} &= v_{ham} \end{aligned} \tag{12}$$

for the hammer, with $\kappa_* = \frac{k}{m}$ the stiffness to mass quotient of the SHO and the hammer respectively. Equation 11 consists of a viscous damping term which heuristically approximated damping parameter γ. The interaction force is computed by relation 17.

8.2 *Wurlitzer Exciter Model*

The reed of the Wurlitzer is modeled as a cantilever beam including large deflection effects, modeled by the inclusion of shearing effects in the beam. Trail and Nash [33] showed that the shear beam is a better approximation for the vibrations of the fundamental frequency then the more popular Euler-Bernoulli beam and less computationally complex than the similar accurate Timoshenko beam model.

The use of a beam model instead of a plate model is justifiable here because torsional motion of the plate were not measured using the high-speed camera setup and thus are either not present or small compared to the transversal deflection of the fundamental mode. In addition to that, the measurements show that the influence of higher modes are comparably small and the mode of vibration could by approximated by the reeds first natural frequency.

The decision to model the vibration of the reed as a 1-dimensional geometry is due to the fact that a larger part of reed influences the electrostatic field as visible in Figs. 2 and 18.

Compared to its height, the deflection of the Wurlitzer's reed is large. Thus it is feasible to include high deflection effects into the formulation of the model. As shown in [34] the inclusion of shear effects to the Euler-Bernoulli beam raises the accuracy of the fundamental frequency as well as the accuracy of higher partials.

Without further derivation we introduce the formulation of the shear beam as developed in [34]. By separating both dependent variables, the deflection and the angle, the equations of transversal motion for a shear beam, given as a partial differential equation can be written as

$$\frac{1}{\rho \mathrm{A}} u_{tt} - \frac{1}{k' \mathrm{GA}} \cdot u_{4x} - \kappa u_{2x2t} - f(x,t) = 0 \tag{13}$$

with $\rho, \mathrm{A}, \mathrm{G}$ dimensionless variables given in Appendix I. Equation 13 does not explicitly depend on the shear angle α (see [34]) thus it is not regarded here any further. Again omitting the shear angle, the boundary conditions for the fixed/free beam are

$$\begin{aligned} u|_0 &= 0 \\ \mathrm{k}' \mathrm{GA} u_x|_L &= 0\ . \end{aligned} \tag{14}$$

8.2.1 Finite Difference Approximation

Again introducing $v = u_t$ and using finite difference operators as defined in Appendix II, it is possible to reduce the PDE 13 to two coupled ordinary differential equations (ODE) thus rewriting the problem as

$$\begin{aligned} \delta_t v &= [\delta_{4x} - \delta_{xx}\delta_{tt}]\mathbf{u} + F([\mathbf{x}], t) \\ \delta_t u &= v \end{aligned} \tag{15}$$

and the boundary conditions as

$$\begin{aligned} u|_0 &= 0 \\ \mathrm{k}' \mathrm{GA} \delta_x u|_L &= 0. \end{aligned} \tag{16}$$

The hammer impact is modeled by using the same impact model presented 17 now including a distributed hammer force over several points on the beam indicated by

$$F([\mathbf{x}], t) = \begin{cases} k \cdot \mathbf{x}(t)^{\alpha} + \lambda \cdot \mathbf{x}(t)^{\alpha} \cdot x_t(t) & \text{if} \quad \sum_{xL} \mathbf{x} > 0 \\ 0 & \text{for} \quad \sum_{xL} \mathbf{x} \leq 0 \end{cases} \tag{17}$$

with $\sum_{xL}$ indicating a weighted sum over the contact area. The time iteration of the hammer motion is again computed by Eq. 12.

8.3 Rhodes Pickup Model

The electromagnetic effects of the Rhodes' pickup system can be reduced from Maxwell's equations for transient electromagnetic effects to a more tractable formulation know as Faraday's law of induction. As shown above, the pickup consists of a magnetized steel tip and a coil wrapped permanent magnet; leaving reciprocal magnetic effects of the induced current in the coil out of our consideration, the voltage induced over the pickup is equivalent to the change of the magnetic flux in the field produced by the magnet

$$\varepsilon = -\frac{\partial \Psi_{\mathbf{B}}}{\partial t} \tag{18}$$

with ε the electromotive force and $\Psi_{\mathbf{B}}$ the magnetic flux due to the change in the magnetic field given by

$$\Psi_{\mathbf{B}} = \int \mathbf{B} \cdot d\mathbf{S} \tag{19}$$

with B the magnetic field strength integrated over surface S. Using these equalities, the induced voltage directly depends on the change of magnetic field strength which depends solely on the position of the tine disturbing the field as shown in Fig. 12.

The following derivation of the magnetic field distribution uses the unphysical assumption that there exist magnetic monopoles which produce a distributed magnetic field.[5] As is shown in [35] this approach yields good approximations of notional magnetic induction fields produced by guitar pickups. Consisting of a plainer geometry, the tip of a guitar pickup bar magnet can be simplified to a circular, magnetically charged disc with a certain cross-section, which reduces the problem to a position-dependent integration of the field over the pickup. Due to the specific pickup geometry of the Rhodes, a different approach is taken here to calculate the induction field strength above the tip of the magnet.

As depicted in Fig. 16 our derivation makes use of several simplifying assumptions facilitating the computation.

Definition 1 The tine vibrates in an approximate sinusoidal motion in one horizontal plane in front of the pickup.

Definition 2 The tip of the tine vibrates on the trajectory of an ideal circle with the center at its fixation point.

[5]This assumption proposes an equivalence between the efficient causes of electric fields and magnetic fields and can be used as a mathematical modeling tool, see: [24, pp. 174 ff].

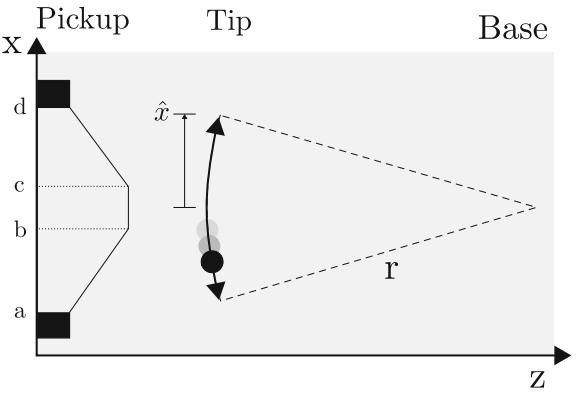

Fig. 16 Simplified geometry of the pickup system and the vibrating tine

Using Definitions 1 and 2, the calculation of the magnetic induction field depending on the position of the tine tip can be formulated as an integral over the simplified iron tip geometry.

Comparable to an electric point charge we define a magnetic point charge which produces a magnetic field given by

$$\mathbf{B} = B_0 \frac{r_{21}}{|r_{21}|^3} \tag{20}$$

with r_{21} the relative positions of the point charge and a test charge in the surrounding field. Because the magnetic flux changes only due to changes in the z direction we can reduce Eq. 20 to

$$\mathbf{B}_z = B_0 \frac{\Delta z}{|r_{21}|^3} \tag{21}$$

The magnetic field for position $(x^{'}, z^{'})$ in front of the of steel tip can thus be written as a three-part integral

$$\begin{aligned} \mathbf{B}_z(x^{'}, z^{'}) = |\mathbf{B}_{tine}| \cdot \Bigg[& \int_a^b \frac{\sigma(z^{'} - z(x))x}{[(x^{'} - x)^2 + (z^{'} - z(x))^2]^{3/2}} dx \\ & + \int_b^c \frac{\sigma(z^{'} - z_k)x}{[(x^{'} - x)^2 + (z^{'} - z_k)^2]^{3/2}} dx \\ & + \int_c^d \frac{\sigma(z^{'} - z(x))x}{[(x^{'} - x)^2 + (z^{'} - z(x))^2]^{3/2}} dx \Bigg] \end{aligned} \tag{22}$$

with σ the constant magnetic charge density.

Integrating this formula for all points on a trajectory given by the position of the Rhodes' tine tip

$$\begin{aligned} z^{'} &= \mathrm{r} - \sqrt{\mathrm{r}^2 - (x^{'})^2} \\ x^{'} &= \hat{\mathrm{x}} \cdot \sin(2\pi f_{tine} t) \end{aligned} \tag{23}$$

with f_{tine} the fundamental frequency of the tine, leads to a magnetic potential function characterising the magnitude of relative magnetic field change.

An idealised form of the magnetic field in front of the Rhodes pickup is depicted in Fig. 17a, b, it is comparable to the measurements results published in [35].

8.4 Wurlitzer Pickup Model

The influence of the pickup system of the Wurlitzer can be characterised in a similar way. Here, the change in capacitance of a time varying capacitor induces an alternating voltage which is amplified as the instruments sound.

A time-varying capacitance induces a current i

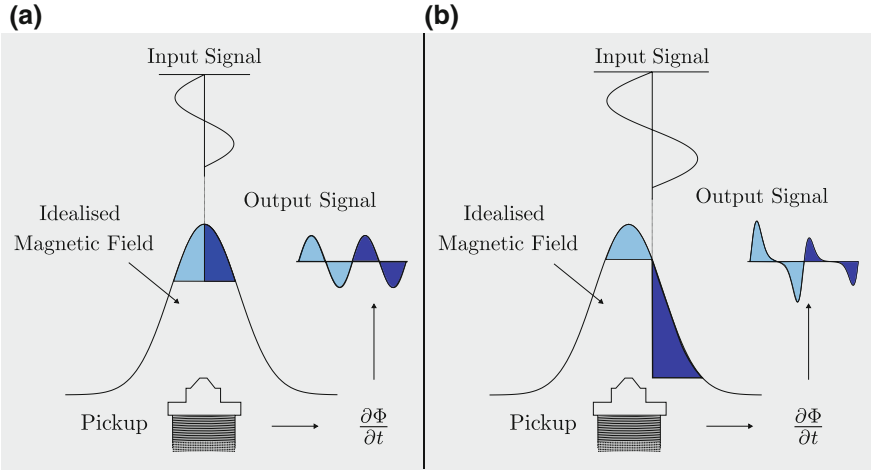

Fig. 17 An idealised schematic depiction of the pickup system of the Rhodes E-piano. The sinusoidal motion of the vibrating tine induces ac. **a** A low amplitude input of a sinusoidal vibration of the magnetic flux weighted by the magnet fields distribution. By differentiating the magnetic flux in respect to time, the alternating voltage present at the output is calculated. **b** A similar model setup as before consisting of a slightly displaced mid-point for the input motion resulting in a different weighting function of the magnetic field. The output shows a different form than before. This condition is close to a realistic playing condition found in Rhodes E-pianos

$$i(t) = \mathrm{C(t)}\frac{\partial \mathrm{u}(t)}{\partial t} + \mathrm{u(t)}\frac{\partial \mathrm{C}(t)}{\partial t} \tag{24}$$

with u the voltage and C the capacitance both depending on time t. For the derivation of the influence function of the capacitor we take two simplifying assumptions.

Definition 3 The time dependent charging/discharging curve of the capacitor is linear in the considered range.

Definition 4 The supply voltage stays constant during a capacity change cycle of the capacitor.

Using Definitions 3 and 4, we can write the time-dependent current resulting from a changing capacitance as

$$i(t) = \mathrm{u}_0 \frac{\partial \mathrm{C}(t)}{\partial t} \tag{25}$$

This alternating current induces an alternating voltage over resistor R_{56}.

To calculate the capacitance curve due to the deflection of the Wurlitzer's reed, a number of i planes through the geometry are taken and the electric field strength is computed for each resulting slice simplifying the 3-dimensional problem to a 1-dimensional. The capacitance for each slice can be computed from the electric field by

$$C_i = \frac{Q_i}{U_i} \tag{26}$$

with $Q_i = \varepsilon_t \oint_A \mathbf{E} \cdot \mathrm{d}\mathbf{A}$ the charge defined as the integral of the electric field over the surfaces of the geometries using Gauss's theorem and ε_t an electric field constant for the material and free field properties.

Three exemplary positions for the computation of the capacitance are depicted in Fig. 18.

8.5 Modeling Results

A structural flow diagram given in Fig. 19 shows that both models share similarities regarding their processing steps. Both models begin by initialising the respective values for the given geometry, then calculating the motion of the respective exciter which is then weighted with a function modeling the spatial distribution of the magnetic or electric field respectively. Both models are implemented in the high-level, high-performance language *julia* and are capable of real-time processing on a second generation medium range Intel i5 processor.

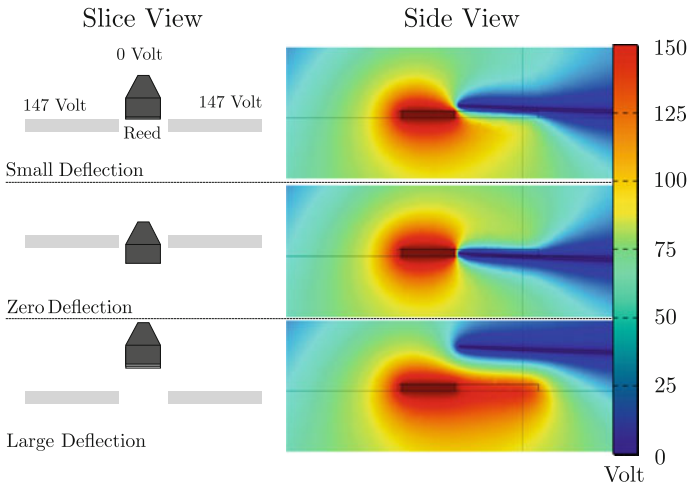

Fig. 18 Distribution of the electric field for three exemplary reed deflections. On the *left hand side* one slice of geometry on the *right hand side* the results from the FEM model

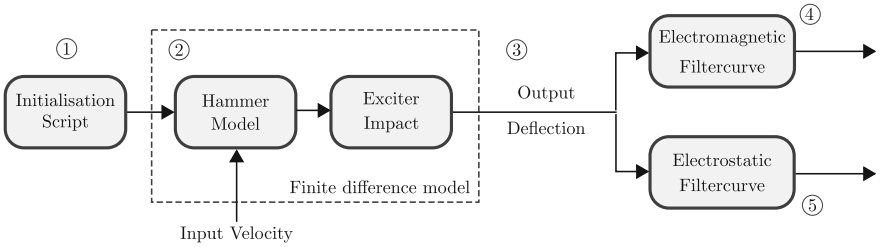

Fig. 19 Schematic depiction of the processing chain of the model. *1* The respective model is initialised regarding its physical properties and boundary condition. *2* Computation of the finite difference models. *3* Output of the respective exciter model. *4* Rhodes model output. *5* Wurlitzer model output

The simulation result for a Rhodes and a Wurlitzer E-piano tone are depicted in Fig. 20. An aural comparison of the simulated and measured sounds shows that both simulations are close to their real counterparts as can be heard on the web-site accompanying this paper.[6] In an informal listening test, which is not part of this publication, the Rhodes' sounds where rated higher than the Wurlitzer sounds pointing to the fact that the complex interaction of the Wurlitzer is approximated less well by the proposed models as the Rhodes' pickup system.

[6]More example sounds can be found on the accompaniment web-site which includes several different examples of exciter to pickup setups. See:http://www.systematicmusicology.de/?page_id=742 .

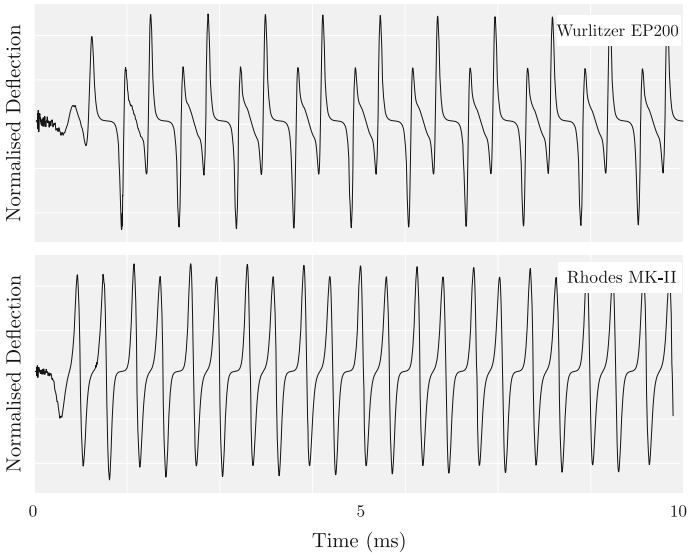

Fig. 20 The first few milliseconds of two simulated keyboard sounds. The full sounds and additional material can be found on the accompanying web-site (ref)

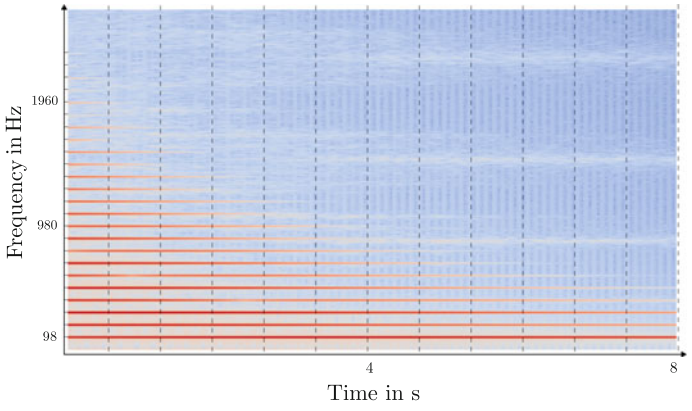

Fig. 21 A spectrogram of the simulated of the Wurlitzer sound

Inspecting the spectrogram of a simulated Wurlitzer sound given in Fig. 21 shows that there are comparably less higher harmonics in the simulated sound and the beating is not as clearly visible as in the measured sound. On the positive side, the beating of the 3rd and 5th harmonic is also present in the simulation even though it is much less pronounced.

9 Outlook

To fill the gap in acoustic research literature this paper was aimed at elucidating the basic sound production components of the Rhodes Stage Piano and the Wurlitzer EP200 series. Hence, other interesting findings are left out of this considerations and are planned to be a part of future publications. Especially interesting is the mechanism of the energy transfer between the Rhodes tine and the Rhodes bar which shows synchronisation behaviour as published in [36, 37]. At the moment, the discourse is only from a heuristic point-of-view and the development of a mathematical model for this non-linear effect is work in progress.

As already mentioned in the derivation of the pickup simulation, a complete model would call for an inclusion of time-varying effects of coupled E-fields and H-fields. Thus, a faithful simulation of these effects using Maxwell's equation of electrodynamics is a work in progress. Our hope is that the nonlinear effects of the Wurlitzer pickups can be represented with higher accuracy, and the missing effects of non-exponential decay and beating can be realised by a more complete model.

Another interesting line of research would be the mechanism of the hammer tine interaction which shows multiple contacts for low notes and high playing force. This is comparable to the effects in piano hammers known from literature.

Another route of research would be a characterisation of the influence of the electric schematics of the Wurlitzer. As the basic change of capacitance is only measurable indirectly the exact influence of the circuit is of interest for comparing the resulting sound.

Even though the Rhodes and Wurlitzer E-pianos are among the most common electro-mechanic keyboard instruments, there exist a multitude of derivatives of similar or comparable tone production principles like for instance the Yamaha CP70/CP80, Hohner *Clavinet*, Hohner *Pianet* or the Hohner *Elektra Piano* to name just a few. A comparison of the primary tone production of those other electromechanical instruments would be a fruitful topic for further considerations.

A conspicuousness that was only mentioned *en passant* in this treatise regards the question why semi-analog or analog-electronic instruments are still preferred among many musicians and listeners and are finding renewed interest over the last years. A psychoacoustic evaluation of important sound parameters in these instruments in regard to listeners' and musicians' preferences could help to answer this question.

9.1 Additional Notes on Electronics

An additional factor influencing the sound of both instruments considerably is the sort of amplification and recording techniques as several classic recordings

show us.[7] The brightness in sound we hear on these recordings are probably produced by the attached amplifiers. Electron tubes and also first/second generation transistors are known to produce a significant percentage of THD even at "clean" level settings. Nevertheless these components are designed to have nearly linear characteristic curves at least at a quiescent operation condition. Furthermore or even more important in the case of the study are aspects of power supply design. The audible compression mentioned above is encouraged by the time-current characteristic of the power supply as well [38]. Both piano sounds have a steep transient followed by a quieter decay of different length of the envelope. The current demand of the transient is to be recovered immediately. The recovery time is longer than the attack response resulting in a longer sustain and a sonic impression of compression, whereby it is the same way an audio compressor acts. Additionally distortion is likely to appear through voltage drop. This behavior is controlled by resistance and capacitance values in the supply itself [39]. Also aging of components and associated rising of Thevenin resistance, loss of capacity and the number, speed and power of simultaneous keystrokes are a control parameters for this phenomenon colloquially known as "voltage sag". The same is true for either amplification circuits and plate voltage load of capacitive pickups respective microphones. So examinations on electronic components influencing musical parameters are fruitful sources for further studies.

10 Conclusion

In this treatise a fundamental consideration of the tone production mechanisms of the Wurlitzer EP200 series and the Rhodes Mark-II electric pianos was presented. We showed that the characteristic timbre of both instruments is due to the specific setup and geometry of the respective pickup systems. A simplified modeling approach for both instruments was proposed showing good accordance with the measured sounds. Both models are able to run in real-time on a not-so-recent personal computer and can be parametrised for different geometries as well as different pickup designs.

It is hoped-for that this work serves as a starting point for further research regarding the acoustic properties of these or other electro-mechanical instruments. Learning about the fundamental mechanisms of those instruments could help to elucidate the fact why the sound of semi-acoustic instruments are still held in such high regards among listeners and musicians.

Acknowledgments It gives us great pleasure to acknowledge the help of Till Weinreich and Martin Keil who helped performing the acoustic and high-speed camera measurements of the Rhodes E-piano.

[7]The Rhodes sounds on the Billy Cobham's track *Snoopy* is a parade example. The keyboarder, Jan Hammer, uses a ring-modulator to modify the instrument sound.

Appendix I

Constants of the shear beam equation introduced in 13. See: [34]:

k' Shape Factor given as $\frac{6(1+v)}{7+6v}$
v Poisson's Ratio
ρ Dimensionless Density
G Dimensionless Shear Modulus
A Dimensionless Area.

Appendix II

FD approximations can be derived by using the fundamental theorem of calculus, which states that the derivative of a variable function $u(x)$ along dimension x is defined by taking the limit of a *finite* difference Δx of the dependent variable Δu like

$$u_x = \lim_{\Delta x \to 0} \frac{\Delta u}{\Delta x}, \tag{27}$$

with u_x indicating a first derivative by x. For non-zeros but small Δx this expression can be utilized to approximate a differential as a difference

$$u_x \approx \delta_x u \tag{28}$$

with Δ_x indicating a centered first order difference operator by x.

This generalized finite difference operator notation is applied throughout the remainder of this work. It is based on the notation used in works like [30, 40, 41].

A discrete shift operator acting on a 1-dimensional function u at position x is indicated by τ with

$$\begin{aligned} \tau_{x+}(u(t,x)) &= u(t, x+\Delta x), \\ \tau_{x-}(u(t,x)) &= u(t, x-\Delta x). \end{aligned} \tag{29}$$

A difference approximation in the forward (+) and backward (−) direction at position x can be written as

$$\begin{aligned} \delta_{x+}\mathbf{u}|_x &= \frac{1}{\Delta x}(u(x+\Delta x) - u(x)) = \frac{1}{\Delta x}(\tau_{x+} - 1)\mathbf{u}, \\ \delta_{x-}\mathbf{u}|_x &= \frac{1}{\Delta x}(u(x) - u(x-\Delta x)) = \frac{1}{\Delta x}(1 - \tau_{x-})\mathbf{u}. \end{aligned} \tag{30}$$

The same can be done in the temporal domain by defining the forward (+) and backward (−) approximation at time instant t as

$$\begin{aligned}\delta_{t+}\mathbf{u}|_t &= \frac{1}{\Delta t}(u(t+\Delta t)-u(t)) = \frac{1}{\Delta t}(\tau_{t+}-1)\mathbf{u},\\ \delta_{t-}\mathbf{u}|_t &= \frac{1}{\Delta t}(u(t)-u(t-\Delta t)) = \frac{1}{\Delta t}(1-\tau_{t-})\mathbf{u}.\end{aligned} \tag{31}$$

An interesting feature of this operator notation is that higher order approximations can be achieved by a convolution of lower order operators. Using (30), a second order centered finite difference operator can be computed by

$$\begin{aligned}\delta_{xx} &= \delta_{x-} * \delta_{x+}\\ &= [\frac{1}{\Delta x}(1-\tau_{-1})] * [\frac{1}{\Delta x}(\tau_+ - 1)]\\ &= \frac{1}{\Delta x^2}(\tau_+ - 1 - 1 + \tau_-)\\ &= \frac{1}{\Delta x^2}(\tau_- - 2 + \tau_+),\end{aligned} \tag{32}$$

with the equivalence $\tau_+ \cdot \tau_- = 1$.

Higher order operators can be calculated similarly

$$\delta_{4x} = \delta_{xx} * \delta_{xx}. \tag{33}$$

References

1. Shear, G., Wright, M.: The electromagnetically sustained Rhodes piano. In: NIME Proceedings, Oslo (2011)
2. Wendland, Torsten: Klang und Akustik des Fender Rhodes E-Pianos. Technische Universität Berlin, Berlin (2009)
3. Rhodes Keyboard Instruments: Service Manual. CBS musical instruments a division of CBS Inc., Fullerton CA (1979)
4. Smith, R.R.: The History of Rickenbacker Guitars, Anaheim CA (1987)
5. Beauchamp, G.D.: Electrical stringed Musical Instrument, US 2089171 A (1934)
6. Donhauser, Peter: Elektrische Klangmaschinen: die Pionierzeit in Deutschland und Österreich. Böhlau Verlag, Wien (2007)
7. Rhodes, H.B.: Electrical Musical Instrument in the Nature of a Piano, U.S. Patent 2,972,922 (1961)
8. Meyer-Eppler, W.: Elektrische Klangerzeugung: elektronische Musik und synthesische Sprache, Bonn (1949)
9. Rhodes, H.B., Woodyard, S.J.: Tuning Fork Mounting Assembly In Electromechnanical Pianos, U.S. Patent 4,373,418 (1983)
10. Andersen, C.W.: Electronic Piano, US 2974555 (1955)
11. Miessner, B.J.: Method and Apparatus for the Production of Music, US Patent 1,929,027 (1931)

12. Vierling, O.: Das elektroakustische Klavier, Berlin (1936).
13. Vierling, O.: Elektrisches Musikinstrument Electric musical instrument, DE1932V0030615 (1937)
14. Duchossoir, A.R.: Gibson Electrics: The Classic Years: An Illustrated History from the Mid-'30s to the mid-'60s. Hal Leonard Corp., Milwaukee, Wis. (1998)
15. Wheeler, Tom: American Guitars: An Illustrated History. Harper, New York (1992)
16. Palkovic, M.: Wurlitzer of Cincinnati: The Name That Means Music To Millions, Charleston (2015)
17. Espinola, S.: Wurlitzer Electric Piano models: a list.|Paleophone. Blog entry Available at: http://paleophone.net/?page_id=923. Accessed 23rd May 2016
18. Rhodes, H.B.: Piano Action, U.S. Patent 4,338,848 (1982)
19. Wurlitzer Company: The Electric Pianos Series 200 and 200A Service Manual. Available at: http://manuals.fdiskc.com/flat/Wurlitzer%20Series%20200%20Service%20Manual.pdf. Accessed 17 Feb 2016
20. Furukawa, T., Tanaka, H., Itoh, H., Fukumoto, H., Ohchi, N.: Dynamic electromagnetic analysis of guitar pickup aided by COMSOL multiphysics. In: Proceedings of the COMSOL Conference Tokyo 2012, Tokyo. COMSOL (2012)
21. Jian-Ming, J.: The Finite Element Method in Electromagnetics, 3rd edn. Wiley, Hoboken. New Jersey (2014)
22. Martin, M.V.: Finite element modelling of the magnetic field of guitar pickups with ANSYS. Master. University of Applied Sciences, Regensburg (2003)
23. Jin, J.: The Finite Element Method in Electromagnetics, 2nd edn. Wiley-IEEE Press, New York (2002)
24. Jackson, J.D.: Classical Electrodynamics, 3rd edn. Wiley, New York (1998)
25. Furukawa, T., Tanaka, H.: Dynamic electromagnetic analysis of guitar pickup aided by COMSOL Multiphysics, Tokyo (2012)
26. Ippolito, A.C.: Electronic piano feedback reduction, US 3435122 A (1965)
27. Avanzini, F., Rocchesso, D.: Physical modeling of impacts: theory and experiments on contact time and spectral centroid. In: Proceedings of the Conference on Sound and Music Computing, pp 287–293 (2004)
28. Stulov, Anatoli: Hysteretic model of the grand piano hammer felt. J. Acoust. Soc. Am. **97**(4), 2577–2585 (1995)
29. Hunt, K.H., Crossley, F.R.E.: Coefficient of restitution interpreted as damping in vibroimpact. J. Appl. Mech. **42**(2), 440–445 (1975)
30. Bilbao, Stefan D.: Numerical Sound Synthesis: Finite Difference Schemes and Simulation in Musical Acoustics. Wiley, Chichester (2009)
31. Pfeifle, F.: Multisymplectic pseudo-spectral finite difference methods for physical models of musical instruments. In: Bader, R. (ed.) Sound—Perception—Performance, volume 1 of Current Research in Systematic Musicology, pp. 351–365. Springer International Publishing (2013)
32. Pfeifle, Florian, Bader, Rolf: Real-time finite-difference method physical modeling of musical instruments using field-programmable gate array hardware. J. Audio Eng. Soc **63**(12), 1001–1016 (2016)
33. Traill-Nash, R.W., Collar, A.R.: the effects of shear flexibility and rotatory inertia on the bending vibrations of beams. Q. J. Mech. Appl. Math. **6**(2), 186–222 (1953)
34. Han, Seon M., Benaroya, Haym, Wei, Timothy: dynamics of transversely vibrating beams using four engineering theories. J. Sound Vib. **225**(5), 935–988 (1999)
35. Horton, Nicholas G., Moore, Thomas R.: Modeling the magnetic pickup of an electric guitar. Am. J. Phys. **77**(2), 144 (2009)
36. Muenster, M., Pfeifle, F.: Non-linear behaviour in sound production of the Rhodes piano. In: Proceedings of the International Symposium of Musical Acoustics (ISMA) 2014, pp. 247–252, Le Mans, France (2014)

37. Muenster, Malte, Pfeifle, Florian, Weinrich, Till, Keil, Martin: Nonlinearities and self-organization in the sound production of the Rhodes piano. J. Acoust. Soc. Am. **136**(4), 2164–2164 (2014)
38. Blencowe, M.: Designing power supplies for tube amplifiers (2010)
39. O'Connor, K.: The Ultimate Tone, vol. 4, Thunderbay (2006). (Chaps. 4–5)
40. Jordan, Charles: Calculus of finite differences, 1st edn. Chelsea Publishing Co, New York (1950)
41. Strikwerda, J.C.: Finite Difference Schemes and Partial Differential Equations, 2nd edn. Society for Industrial and Applied Mathematics, Philadelphia, USA (2004)

Author Biographies

Florian Pfeifle received his M.A. in systematic musicology and electrical engineering in 2010 and his Ph.D. in 2014. His current research is concerned with real-time grand piano physical modeling on FPGAs. Additionally, he is interested in instrument acoustics, scientific computation, and jazz music research. Until recently, he worked also as a musician/producer being awarded gold records for two of his works.

Malte Münster studied musicology, psychology, and phonetics. In addition, he studied piano, guitar and composition. He holds a Master's degree in Systematic Musicology and currently completes a Ph.D.-thesis in the field of musical acoustics with a focus on bronze metallophones. He did ethnomusicological fieldwork in Brazil and in areas of the Balkan Peninsula where he recorded a wide range of rural styles. Malte Münster is also active as an engineer and producer recording various artists in his studio.